Macromolecules
ARTICLE

Macromolecules **2010**, *43*, 821–826 **821**
DOI: 10.1021/ma902398q

Diketopyrrolopyrrole-Based Semiconducting Polymer for Photovoltaic Device with Photocurrent Response Wavelengths up to 1.1 μm

Erjun Zhou,[†] Qingshuo Wei,[‡] Shimpei Yamakawa,[‡] Yue Zhang,[‡] Keisuke Tajima,[‡] Chunhe Yang,[†] and Kazuhito Hashimoto*,[†,‡]

[†]*HASHIMOTO Light Energy Conversion Project, ERATO, Japan Science and Technology Agency (JST) and* [‡]*Department of Applied Chemistry, School of Engineering, The University of Tokyo, 7-3-1 Hongo, Bunkyo-ku, Tokyo 113-8656, Japan*

Received October 29, 2009; Revised Manuscript Received December 1, 2009

ABSTRACT: A highly effective photovoltaic polymer with near-infrared response, poly{*N*-[1-(2-ethylhexyl)-3-ethylheptanyl]-dithieno[3,2-*b*:2′,3′-*d*]pyrrole-3,6-dithien-2-yl-2,5-dibutylpyrrolo[3,4-*c*]pyrrole-1,4-dione-5′,5″-diyl} {PDTP-DTDPP(Bu)}, was synthesized. The polymer has high molecular weight, good solubility, and a broad absorption spectrum in the range of 500−1100 nm. Field effect transistor charge mobility of PDTP-DTDPP(Bu) arrived 0.05 $cm^2 V^{-1} s^{-1}$. Bulk heterojunction type polymer solar cells based on PDTP-DTDPP(Bu) and $PC_{70}BM$ have broad photocurrent response wavelength range from 300 nm to 1.1 μm. High short-circuit current (14.87 mA/cm^2) and power conversion efficiency (2.71%) were achieved, which is a significant advance for efficient photovoltaic polymers that respond to the whole range of the solar spectrum.

Introduction

In the past decade, polymer solar cells (PSCs) have received a great deal of attention as a potential renewable energy source due to their potential advantages such as low fabrication cost, light weight, and fast production of large area devices by roll-to-roll solution processes.[1] Among photovoltaic polymers, regioregular poly(3-hexylthiophene) (P3HT) has been extensively studied. Bulk heterojunction (BHJ) photovoltaic device combining P3HT as the electron donor with [6,6]-phenyl C_{61} butyric acid methyl ester (PCBM) as the electron acceptor have achieved power conversion efficiencies (PCEs) as high as 4−5%.[2] However, the upper limit seems to have been reached for this material combination, as P3HT utilizes only photons located in the high-energy fraction of the solar spectrum with wavelengths below 650 nm. In fact, ∼40% of the total solar energy lies in the range of 650−1100 nm, which is a strong driving force for developing low-bandgap polymers to utilize the solar energy in the near-infrared (NIR) range.[3]

Recently, significant progress has been made in the photovoltaic application of novel low-bandgap polymers with optical absorption wavelengths in the range of 700−900 nm.[4] Nevertheless, design of efficient photovoltaic polymers with optical absorption and photocurrent response extending to wavelengths of micrometers remains challenging. The first example of this kind of micrometer-response polymer (μmR-polymer) was APFO-Green1, reported by Inganäs et al. in 2004.[5] Subsequently, considerable effort has been devoted to the design and synthesize of μmR-polymers via a synthetic strategy of combining electron-rich units (donors) and electron-deficient units (acceptors) in a copolymer main chain. To date, no more than 10 μmR-polymers have been synthesized, which are primarily based on a very strong electron-deficient unit such as [1,2,5]thiadiazolo[3,4-*g*]quinoxaline,[6] thienopyrazine,[7] or thieno[3,4-*c*][1,2,5]thiadiazole.[8] The photocurrent response of all of these polymers extends to a wavelength of 1 μm; however, the external quantum efficiency (EQE) of these PSCs in the wavelength range between 650 and 1100 nm is typically less than 10%, which results in low overall PCEs under AM1.5 simulated solar light. Up to now, the highest PCE of μmR-polymer was just 1.1%, based on poly(di-2-thienylthienopyrazine) by using complicated doubled active layers photovoltaic devices.[7]

The fundamental requirements for promising photovoltaic μmR-polymers include the following: (a) broad absorption extending to or surpassing 1 μm to absorb more sunlight; (b) a high LUMO energy level to allow effective photoinduced charge transfer from the polymers to the acceptor in the BHJ device and at the same time, a low HOMO level to keep the open circuit voltage (V_{OC}) as high as possible; (c) high carrier mobility to ensure that effective charge carrier transport to the electrodes suppresses photocurrent loss; and (d) good solubility and appropriate compatibility with fullerene derivatives to form high-quality films by solution processing. The lack of successful photovoltaic μmR-polymers might be due to the difficulty of fulfilling all these requirements simultaneously with one polymer.

Very recently, 3,6-dithien-2-yl-2,5-dialkylpyrrolo[3,4-*c*]pyrrole-1,4-dione (DTDPP) was shown to be a promising building block for the design of photovoltaic polymers.[9] In our previous work, we also found the polymer, PDTP-DTDPP, based on DTDPP and dithieno[3,2-*b*:2′,3′-*d*]pyrrole was one of potential μmR-polymers. The PCE based on this polymer arrived 1.1%, one of highest value for μmR-polymers.[10] Herein, we present a new donor−acceptor alternative conjugated polymer, changing the alkyl chain in the diketopyrrolopyrrole segment of PDTP-DTDPP from 2-ethylhexyl to *n*-butyl. This new polymer, referred to as PDTP-DTDPP(Bu), is designed to fulfill the above-mentioned requirements simultaneously as much as possible. As a result, bulk heterojunction-type polymer solar cells based on PDTP-DTDPP(Bu) and $PC_{70}BM$ have broad photocurrent response wavelength range from 300 nm to 1.1 μm. High short-circuit current (14.87 mA/cm^2) and PCE (2.71%) were achieved, which is a significant advance for efficient μmR-polymers.

*Corresponding author. E-mail: hashimoto@light.t.u-tokyo.ac.jp.

Published on Web 12/28/2009

Scheme 1. Synthetic Routes for Monomers and PDTP-DTDPP(Bu)

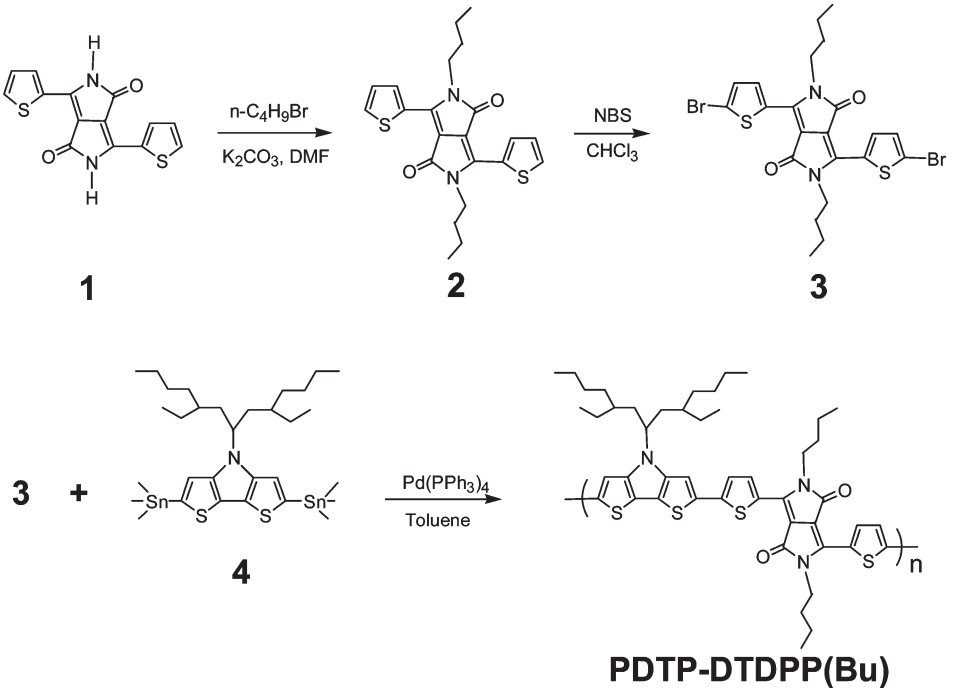

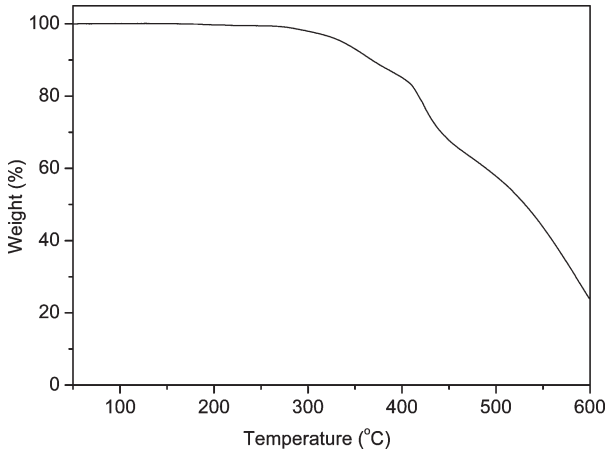

Figure 1. TGA plot of PDTP-DTDPP(Bu).

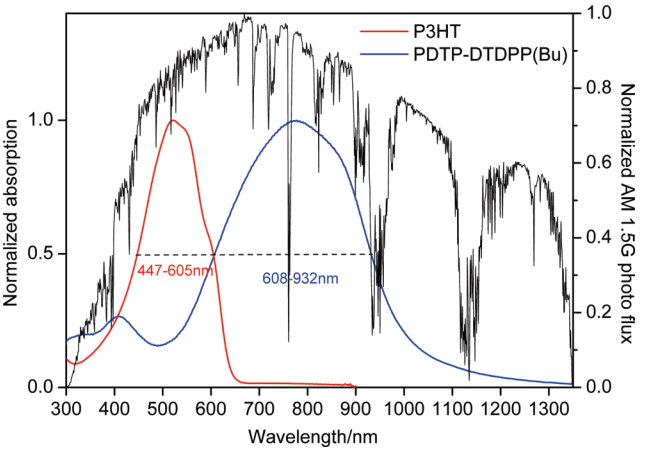

Figure 2. Normalized absorption spectra of PDTP-DTDPP(Bu) and P3HT films spin-coated on quartz plates from $CHCl_3$ solution.

Results and Discussion

Material Synthesis. The new polymer PDTP-DTDPP(Bu) was synthesized by coupling 3,6-di(2-bromothien-5-yl)-2,5-dibutylpyrrolo[3,4-*c*]pyrrole-1,4-dione and 2,6-di(trimethyltin)-*N*-[1-(2′-ethylhexyl)-3-ethylheptanyl]dithieno[3,2-*b*:2′,3′-*d*]-pyrrole via a Stille reaction (Scheme 1). The polymer has good solubility in $CHCl_3$ but is only partly soluble in chlorobenzene and *o*-dichlorobenzene. The number-average molecular weight (M_n) of the polymer is 18.9 kg/mol with a polydispersity index (PDI) of 2.04. Thermogravimetric analysis (TGA) plots of PDTP-DTDPP(Bu) is shown in Figure 1. The polymer exhibits excellent stability with an onset decomposition temperature (1% weight loss) at 280 °C in air. This level of thermal stability is adequate for applications in PSCs and other optoelectronic devices.

Optical Properties. The absorption spectrum of PDTP-DTDPP(Bu) in film is shown in Figure 2 together with that of P3HT and normalized AM 1.5G photon flux for comparison. The polymer has a broad absorption band in the range of 500−1100 nm with a tail extending to 1.3 μm. The full width at half-maximum (fwhm) of PDTP-DTDPP(Bu) film is 324 nm, which is nearly a double that of P3HT film (158 nm). The optical band gap of the PDTP-DTDPP(Bu) film is 1.13 eV, as estimated from the absorption onset (1100 nm). All these data indicate that PDTP-DTDPP(Bu) can utilize a larger fraction of solar light that P3HT as a possible material for applications in micrometer response photovoltaic devices.

Electrochemical Properties. Electrochemical cyclic voltammetry (CV) was performed to determine the highest occupied molecular orbital (HOMO) and lowest unoccupied molecular orbital (LUMO) energy levels of PDTP-DTDPP(Bu). The CV curves were recorded referenced to an Ag/Ag^+ electrode, which was calibrated against the ferrocene−ferrocenium (Fc/Fc^+) redox couple (4.8 eV below the vacuum level); the CV curves are shown in Figure 3. On the basis of the onset values of oxidation (0.10 V) and reduction potential (−1.17 V) of the polymer, the HOMO and LUMO levels of the polymer were calculated as −4.90 and −3.63 eV,

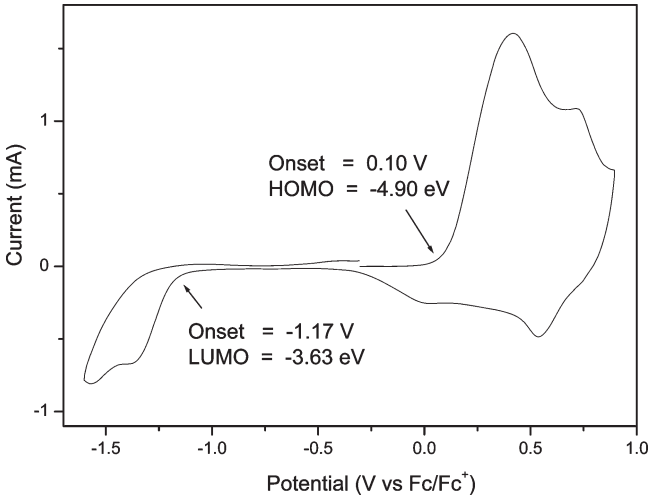

Figure 3. Cyclic voltammogram of polymer film on platinum plate in acetonitrile solution of 0.1 mol/L $[Bu_4N]PF_6$ (Bu = butyl) at scan rate of 50 mV/s.

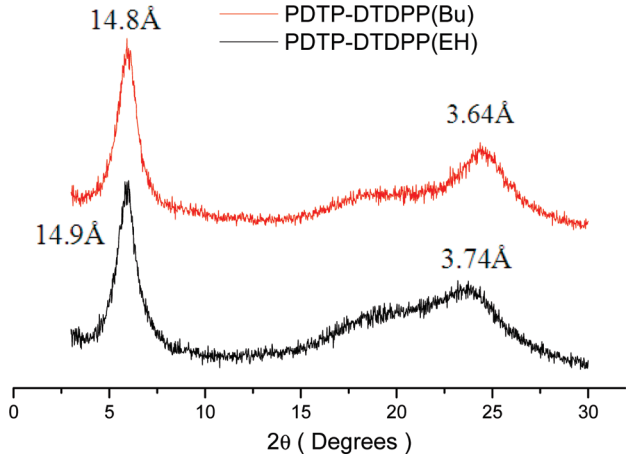

Figure 4. XRD patterns of the bulk samples of PDTP-DTDPP(Bu) and PDTP-DTDPP(EH).

respectively. The electrochemical band gap thus determined is about 1.27 eV, which is slightly higher than the optical band gap.

X-ray Diffraction (XRD) Measurements. The XRD patterns of the bulk samples of PDTP-DTDPP(Bu) and PDTP-DTDPP(EH) were recorded to understand their structures in the solid state. As shown in Figure 4, both samples show diffraction peaks at low angles, which could be attributed to a lamellar structure. The *d*-spacings of the diffraction from (100) are 14.8 and 14.9 Å for PDTP-DTDPP(Bu) and PDTP-DTDPP(EH), respectively. The peaks around 24° for both polymers can be assigned to the face-to-face distance of the aromatic groups in the polymer chains arranged in the parallel direction. This $\pi-\pi$ stacking distance of PDTP-DTDPP(Bu) was 3.64 Å, slightly lower than that of PDTP-DTDPP(EH) (3.74 Å), which suggests that the butyl group in DPP segment is better for the close $\pi-\pi$ stacking of the polymer backbones compared to the bulkier 2-ethylhexyl group.

Hole Mobility. It has been strongly suggested that high hole mobility is an important requirement for effective photovoltaic polymers.[11] The mobility of PDTP-DTDPP-(Bu) was measured by using a field-effect transistor (FET) with a bottom-gate, top-contact device configuration built

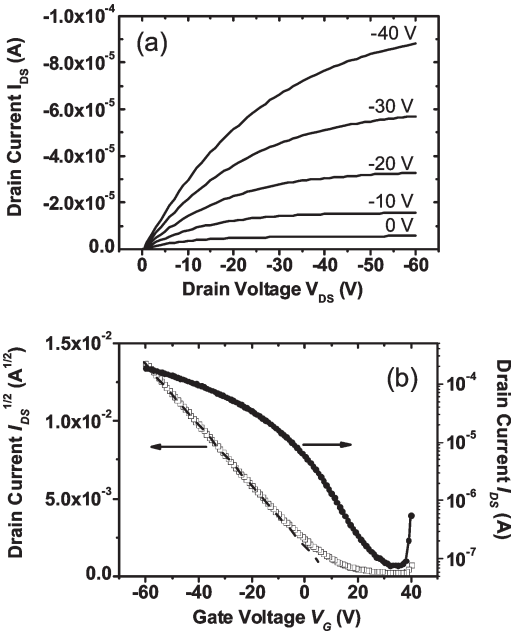

Figure 5. FET characteristics of an exemplary OFET with PDTP-DTDPP(Bu) on OTS-modified substrate (channel length = 50 μm, channel width = 8 mm): (a) output curves at different gate voltages and (b) transfer curve in saturated regime at constant source-drain voltage of −40 V and square root of the absolute value of current as a function of gate voltage.

on an n-doped silicon wafer. Figure 5 shows the typical output and transfer curves of a representative device with PDTP-DTDPP(Bu) as the channel semiconductor. The hole mobility was estimated to be 0.05 $cm^2\ V^{-1}\ s^{-1}$, which is 1−2 orders of magnitude higher than that of other effective D−A type low-bandgap photovoltaic polymers (2.6×10^{-4}−3×10^{-3} $cm^2\ V^{-1}\ s^{-1}$).[5] Although the FET mobility might not be directly correlated to the photovoltaic performance since the situation of the charge transport is quite different from each other, the higher carrier mobility still suggests effective charge carrier transport to the electrodes in the photovoltaic devices.

Photovoltaic Properties. The bulk heterojunction PSCs were fabricated with the device structure of ITO/PEDOT:PSS/PDTP-DTDPP(Bu):PCBM (or $PC_{70}BM$)/LiF/Al. PEDOT:PSS was spin-coated on a precleaned ITO-coated glass substrate. The film was dried at 150 °C under a N_2 atmosphere for 5 min. After cooling the substrate, a solution of PDTP-DTDPP(Bu) and PCBM (or $PC_{70}BM$) mixture (1:2 w/w) was spin-coated, where a blend of chloroform and *o*-dichlorobenzene (4:1 v/v) was used as the solvent. The devices were completed by evaporating LiF/Al as the cathode. The effective area (2 mm × 3 mm) of the PSCs was defined using a metal photomask during irradiation with simulated solar light (Scheme 2).

$PC_{70}BM$ was also used as an acceptor because it has similar electronic properties as PCBM, but a higher absorption coefficient in the visible region, which can compensate for the poor absorption of PDTP-DTDPP(Bu) in this range. Figure 6 shows the $I-V$ curves of the devices with the best photovoltaic performance under the illumination of AM 1.5 (100 mW/cm^2). The corresponding open-circuit voltage (V_{OC}), short-circuit current (I_{SC}), fill factor (FF), and PCE of the devices are also summarized in Figure 3. The external quantum efficiency (EQE) of the devices under the illumination of monochromatic light is shown in Figure 3. Compared with the PDTP-DTDPP(Bu):PCBM system, the

Scheme 2. Schematic Representation of Bulk Heterojunction PSCs and Molecular Structures of PDTP-DTDPP(Bu) and Fullerene Derivatives

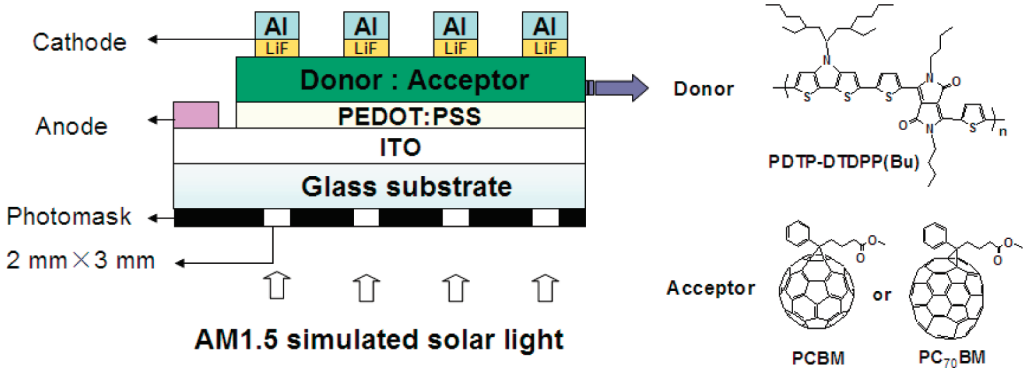

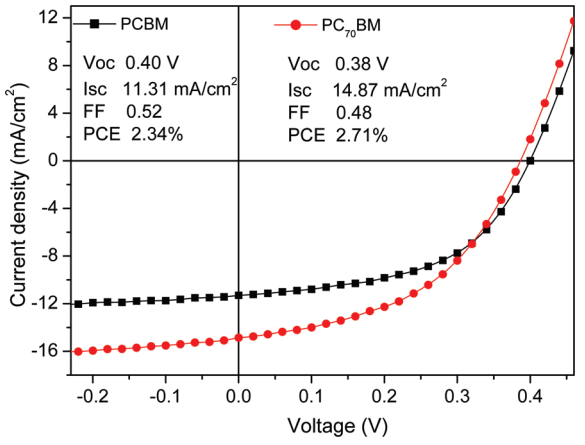

Figure 6. $I-V$ curves of PSCs based on bulk heterojunction of PDTP-DTDPP(Bu) with PCBM or $PC_{70}BM$ under illumination of AM 1.5, 100 mW/cm^2.

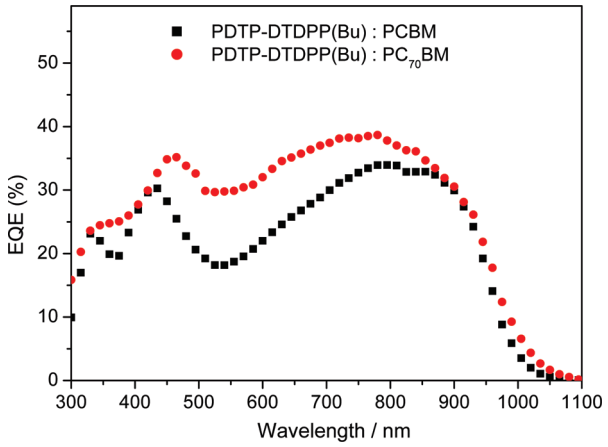

Figure 7. EQE spectra of PSCs based on PDTP-DTDPP(BU) with PCBM or $PC_{70}BM$.

PDTP-DTDPP(Bu):$PC_{70}BM$ system has higher EQE values of 30−40% in the range of 450−850 nm, which contributes to the improvement of I_{SC} from 11.31 to 14.87 mA/cm^2. Since the spectral response extends to over 1.1 μm, the spectral mismatch between the simulated and actual AM1.5 spectra must be considered. We compared the experimental I_{SC} under the simulated AM1.5 irradiation and the I_{SC} calculated by integrating the EQE and the actual AM1.5 solar spectra. The calculated I_{SC} from the EQE was 15% less than the measured I_{SC}. This discrepancy might be attributed to the spectral mismatch in the NIR region and/or device degradation during measurements in air.

The highest PCE of PSCs based on the PDTP-DTDPP-(Bu):$PC_{70}BM$ system reached 2.71%, which was lower than the 4−5% of the P3HT:PCBM devices. This could be mainly attributed to the lower V_{OC} (~0.4 V). In addition, the charge separation efficiency in the current combination might not be as high as that in P3HT:PCBM, although it was difficult to estimate the internal quantum efficiency (IQE) accurately due to the light interference effect in the films. This might be attributed to the smaller LUMO offset or less ideal mixing morphology between the polymer and PCBM. Nevertheless, this performance is more than double of the highest PCE (1.1%) reported to date for μmR-polymers, even when the spectral mismatch in the NIR region above was considered. Such improvement of PCE comes from relatively high-efficiency photon-to-electron conversion in the broad range of the absorption in the blend film of PDTP-DTDPP(Bu) and PCBM. Considering the high EQE obtained in the range from 650 to 950 nm, PDTP-DTDPP(Bu) is a promising candidate for applications in tandem photovoltaic devices in combination with conventional visible light absorbing materials. Furthermore, comparing the photovoltaic performance of PDTP-DTDPP(Bu) with PDTP-DTDPP(EH) suggests that the alkyl chain in the DPP segment has a large influence on the photovoltaic properties of the polymers. A similar phenomenon was also observed for other D−A type photovoltaic polymers.[12] Synthesis of new μmR-polymers with different alkyl chain in both the DTDPP segment and the dithieno[3,2-*b*:2′,3′-*d*]pyrrole segment and a detailed comparison of the properties of all these polymers are now in progress.

The energy loss from the low output voltage of the photovoltaic devices (0.38−0.4 V) can be attributed to the relatively large difference between the LUMO levels of PDTP-DTDPP(Bu) and PCBM (i.e., small energy difference between the HOMO of PDTP-DTDPP(Bu) and LUMO of PCBM). There is still a room to lower the LUMO level of PDTP-DTDPP(Bu) from 3.63 to ~4.0 eV, which is ~0.3 eV higher than the LUMO level of PCBM. If we can control the mixing morphology suitable for the charge separation, this energy offset might be enough to maintain a sufficient driving force for charge transfer and the higher V_{OC} could be expected at the same time. Further fine-tuning of the LUMO and HOMO levels of the polymer by structural modification may improve V_{OC} and promote the utilization of more NIR light by the lower bandgap materials.

Conclusion

In conclusion, a highly effective photovoltaic polymer with NIR response, PDTP-DTDPP(Bu), based on alternating *N*-[1-(2-ethylhexyl)-3-ethylheptanyl]dithieno[3,2-*b*:2′,3′-*d*]pyrrole and

3,6-dithien-2-yl-2,5-dibutylpyrrolo[3,4-*c*]pyrrole-1,4-dione units has been synthesized. PDTP-DTDPP(Bu) has high hole mobility ($0.05\ cm^2\ V^{-1}\ s^{-1}$) and broad photocurrent response wavelengths from 300 nm to 1.1 μm. The photovoltaic properties of PDTP-DTDPP(Bu) were preliminarily investigated, and high short-circuit current ($14.87\ mA/cm^2$) and PCE (2.71%) were achieved. Considering the sufficiently high I_{SC} values of this system, more promising photovoltaic performance is thought to be achievable by using other fullerene derivatives with high LUMO energy levels, such as bis-PCBM[13] or Lu3N@C80-PCBH.[14] Further device optimization and the synthesis of new μmR-polymers are currently in progress and will be reported in due course.

Experimental Section

Synthesis. All the chemicals were purchased from Alfa, Aldrich, or Wako and used without further purification. The following compounds were synthesized according to procedures in the literature: 3,6-dithien-2-yl-2,5-dihydropyrrolo[3,4-*c*]pyrrole-1,4-dione (**1**)[15] and 2,6-di(trimethyltin)-*N*-[1-(2′-ethylhexyl)-3-ethylheptanyl]dithieno[3,2-*b*:2′,3′-*d*]pyrrole (**4**).[16]

3,6-Dithien-2-yl-2,5-dibutylpyrrolo[3,4-*c*]pyrrole-1,4-dione (2). Monomer **1** (2.4 g, 8 mmol), K_2CO_3 (3.3 g, 24 mmol), and DMF (80 mL) were added to a 200 mL double-neck round-bottom flask. The reaction container was purged with N_2 for 20 min and heated to 120 °C for 1 h. 1-Bromobutane (2.4 mL, 22.4 mmol) was added dropwise by syringe, and the reaction mixture was stirred for 24 h at 130 °C. The solution was cooled to room temperature, poured into 200 mL of water, and stirred for 30 min. The water layer was extracted with $CHCl_3$, and the combined organic layers were dried over $MgSO_4$ and the solvents were removed by rotary evaporation. Finally, the crude compound was purified by column chromatography (silica gel; eluent: chloroform/hexane 1/1 (v/v)) and isolated as a purple-brown solid. Yield: 2.7 g (82%). ^{1}H NMR ($CDCl_3$, 400 MHz): δ (ppm) 8.92 (d, 2H), 7.64 (d, 2H), 7.29 (t, 2H), 4.09 (t, 4H), 1.74 (m, 4H), 1.43 (m, 4H), 0.97 (t, 6H). MALDI-TOF MS (m/z) 412.19 (M^+).

3,6-Di(2-bromothien-5-yl)-2,5-dibutylpyrrolo[3,4-*c*]pyrrole-1,4-dione (3). In a 500 mL round-bottom flask, compound **2** (1.65 g, 4 mmol) was dissolved in 250 mL of $CHCl_3$, and the flask was covered with aluminum foil. *N*-Bromosuccinimide (1.57 g, 8.8 mmol) was added portionwise, and the reaction mixture was stirred for 48 h at room temperature. After that, the reaction mixture was poured into water, and the organic phase was separated and washed by water. The organic layers were dried over $MgSO_4$ and concentrated by rotary evaporation. The crude compound was purified by column chromatography (silica gel; eluent: chloroform/hexane 1/1 (v/v)), and the title compound was isolated as a dark-purple solid. Yield: 1.7 g (75%). ^{1}H NMR ($CDCl_3$, 400 MHz): δ (ppm) 8.69 (d, 2H), 7.24 (d, 2H), 4.00 (t, 4H), 1.71 (m, 4H), 1.46 (m, 4H), 0.98 (t, 6H). MALDI-TOF MS (m/z) 570.03 (M^+).

Poly{*N*-[1-(2-ethylhexyl)-3-ethylheptanyl]dithieno[3,2-*b*:2′,3′-*d*]-pyrrole-3,6-dithien-2-yl-2,5-dibutylpyrrolo[3,4-*c*]pyrrole-1,4-dione-5′,5″-diyl} {PDTP-DTDPP(Bu)}. Monomer **2** (201.4 mg, 0.353 mmol), monomer **3** (262.5 mg, 0.353 mmol), and dry toluene (15 mL) were added to a 50 mL double-neck round-bottom flask. The reaction container was purged with N_2 for 30 min to remove O_2. $Pd(PPh_3)_4$ (5%, 20 mg) was added, and the reaction mixture was heated to 110 °C. The solution was stirred at 110 °C for 48 h. The resulting dark blue sticky solution was cooled to room temperature and poured into methanol (200 mL), and the precipitates were collected by filtration and then washed with methanol. The solid was dissolved in $CHCl_3$ (150 mL) and passed through a column packed with alumina, Celite, and silica gel. The column was eluted with $CHCl_3$. The combined polymer solution was concentrated and poured into methanol, after which the precipitates were collected and dried. Yield: 250 mg (86%). ^{1}H NMR ($CDCl_3$, 400 MHz): δ (ppm) 9.00 (br, 2H), 7.5−6.8 (m, 4H), 4.50 (br, 1H), 4.10 (br, 4H), 2.1−0.6 (m, 48H). M_n = 18.9 kg/mol; polydispersity = 2.04.

Characterization. ^{1}H NMR (400 MHz) spectra were measured using a JEOL Alpha FT-NMR spectrometer equipped with an Oxford superconducting magnet system. Absorption spectra were measured using a Shimadzu MPC-3100 spectrophotometer. Cyclic voltammograms (CVs) were recorded on an HSV-100 (Hokuto Denkou) potentiostat. A Pt plate coated with a thin polymer film was used as the working electrode. A Pt wire and an Ag/Ag^+ (0.01 M of $AgNO_3$ in acetonitrile) electrode were used as the counter and the reference electrodes (calibrated against Fc/Fc^+), respectively. X-ray diffraction (XRD) patterns were recorded on a Rigaku RCD-2400H diffractometer.

Fabrication and Characterization of Field-Effect Transistor. Transistors were built on highly doped n-type (100) Si substrates (< 0.02 Ω cm) with 300 nm thermally grown silicon dioxide. Octadecyltrichlorosilane (OTS) SAM was formed by soaking the substrates in a 5 mM toluene solution of OTS for 12 h in a dry N_2-filled glovebox. The capacitance of the gate dielectric was $C_i = 10.7\ nF\ cm^{-2}$. Chloroform solution of the polymer (5 mg mL^{-1}) was directly spin-coated onto the dielectric substrates (3000 rpm, 30 s). After the films were thermally annealed at 150 °C for 10 min, gold electrodes (L = 50 μm and W = 8 mm) were evaporated onto the surface through a metal mask. The electrical characteristics of the transistors were measured using Keithley 2400 and 6430 source/measurement units at room temperature. All the transistors were measured under ambient conditions.

Fabrication and Characterization of Polymer Solar Cells. PSCs were constructed in the traditional sandwich structure through several steps. ITO-coated glass substrates were cleaned by ultrasonication sequentially in detergent, water, acetone, and 2-propanol. After drying the substrate, PEDOT:PSS (Baytron P) was spin-coated (4000 rpm for 30 s) on ITO. The film was dried at 150 °C under a N_2 atmosphere for 5 min. After cooling the substrate, a chloroform and *o*-dichlorobenzene (4:1 v/v) solution of the polymer and PCBM mixture (1:2 w/w) was spin-coated. After drying the solvent, the substrate was transferred into an evaporation chamber (ALS technology H-2807 vacuum evaporation system with E-100 load lock). LiF (~1 nm)/Al (~60 nm) electrode was evaporated onto the substrate under high vacuum (10^{-4}−10^{-5} Pa). Postdevice annealing was carried out at 110 °C for 5 min inside a nitrogen-filled glovebox. The current−voltage characteristics of the photovoltaic cells were measured using a Keithley 2400 I−V measurement system. The measurements were conducted under the irradiation of AM 1.5 simulated solar light (100 mW cm^{-2}, Peccell Technologies PCE-L11). Light intensity was adjusted by using a standard silicon solar cell with an optical filter (Bunkou Keiki BS520). The external quantum efficiency (EQE) of the devices was measured on a Hypermonolight System (Bunkou Keiki SM-250F).

References and Notes

(1) (a) Brabec, C. J.; Sariciftci, N. S.; Hummelen, J. C. *Adv. Funct. Mater.* **2001**, *11*, 15. (b) Coakley, K. M.; McGehee, M. D. *Chem. Mater.* **2004**, *16*, 4533. (c) Shaheen, S. E.; Ginley, D. S.; Jabbour, G. E. *MRS Bull.* **2005**, *30*, 10. (d) Günes, S.; Neugebauer, H.; Sariciftci, N. S. *Chem. Rev.* **2007**, *107*, 1324. (e) Thompson, B. C.; Fréchet, J. M. J. *Angew. Chem., Int. Ed.* **2008**, *47*, 58.

(2) (a) Li, G.; Shrotriya, V.; Huang, J. S.; Yao, Y.; Moriarty, T.; Emery, K.; Yang, Y. *Nat. Mater.* **2005**, *4*, 864. (b) Ma, W. L.; Yang, C. Y.; Gong, X.; Lee, K.; Heeger, A. J. *Adv. Funct. Mater.* **2005**, *15*, 1617.

(3) (a) Winder, C.; Sariciftci, N. S. *J. Mater. Chem.* **2004**, *14*, 1077. (b) Bundgaard, E.; Krebs, F. C. *Sol. Energy Mater. Sol. Cells* **2007**, *91*, 954. (c) Li, Y. F.; Zou, Y. P. *Adv. Mater.* **2008**, *20*, 2952.

(4) (a) Peet, J.; Kim, J. Y.; Coates, N. E.; Ma, W. L.; Moses, D.; Heeger, A. J.; Bazan, G. C. *Nat. Mater.* **2007**, *6*, 497. (b) Hou, J. H.; Chen, H. Y.; Zhang, S. Q.; Li, G.; Yang, Y. *J. Am. Chem. Soc.* **2008**, *130*, 16144. (c) Liang, Y. Y.; Feng, D. Q.; Wu, Y.; Tsai, S.-T.; Li, G.; Ray, C.; Yu, L. P. *J. Am. Chem. Soc.* **2009**, *131*, 7792. (d) Park, S. H.;

Roy, A.; Beaupré, S.; Cho, S.; Coates, N.; Moon, J. S.; Moses, D.; Leclerc, M.; Lee, K.; Hegger, A. J. *Nat. Photonics* **2009**, *3*, 297.
(5) Wang, X. J.; Perzon, E.; Delgado, J. L.; de la Cruz, P.; Zhang, F. L.; Langa, F.; Andersson, M.; Inganäs, O. *Appl. Phys. Lett.* **2004**, *85*, 5081.
(6) (a) Wang, X. J.; Perzon, E.; Oswald, F.; Langa, F.; Admassie, S.; Andersson, M. R.; Inganäs, O. *Adv. Funct. Mater.* **2005**, *15*, 1665. (b) Wang, X. J.; Perzon, E.; Mammo, W.; Oswald, F.; Admassie, S.; Persson, N.-K.; Langa, F.; Andersson, M. R.; Inganäs, O. *Thin Solid Films* **2006**, *511*−*512*, 576. (c) Perzon, E.; Zhang, F. L.; Andersson, M.; Mammo, W.; Inganäs, O.; Andersson, M. R. *Adv. Mater.* **2007**, *19*, 3308. (d) Yi, H. N.; Johnson, R. G.; Iraqi, A.; Mohamad, D.; Royce, R.; Lidzey, D. G. *Macromol. Rapid Commun.* **2008**, *29*, 1804. (e) Zoombelt, A. P.; Fonrodona, M.; Wienk, M. M.; Sieval, A. B.; Hummelen, J. C.; Janssen, R. A. J. *Org. Lett.* **2009**, *11*, 903.
(7) (a) Wienk, M. M.; Turbiez, M. G. R.; Struijk, M. P.; Fonrodona, M.; Janssen, R. A. J. *Appl. Phys. Lett.* **2006**, *88*, 153511.
(8) Xia, Y. L.; Wang, L.; Deng, X. Y.; Li, D. Y.; Zhu, X. H.; Cao, Y. *Appl. Phys. Lett.* **2006**, *89*, 81106.
(9) (a) Wienk, M. M.; Turbiez, M.; Gilot, J.; Janssen, R. A. J. *Adv. Mater.* **2008**, *20*, 2556. (b) Zou, Y. P.; Gendron, D.; Badrou-Aïch, R.; Najari, A.; Tao, Y.; Leclerc, M. *Macromolecules* **2009**, *42*, 2891. (c) Zou, Y. P.; Gendron, D.; Neagu-Plesu, R.; Leclerc, M. *Macromolecules* **2009**, *42*, 6361. (d) Huo, L. J.; Hou, J. H.; Chen, H. Y.; Zhang, S. Q.; Jiang, Y.; Chen, T. L.; Yang, Y. *Macromolecules* **2009**, *42*, 6564. (e) Yu, C.-Y.; Chen, C.-P.; Chan, G.-H.; Hwang, G.-W.; Ting, C. *Chem. Mater.* **2009**, *21*, 3262. (f) Bijleveld, J. C.; Zoombelt, A. P.; Mathijssen, S. G. J.; Wienk, M. M.; Turbiez, M.; de Leeuw, D. M.; Janssen, R. A. J. *J. Am. Chem. Soc.* **2009**, *131*, 16616.
(10) Zhou, E. J.; Yamakawa, S.; Tajima, K.; Yang, C. H.; Hashimoto, K. *Chem. Mater.* **2009**, *21*, 4055.
(11) Chen, J. W.; Cao, Y. *Acc. Chem. Res.* **2009**, *42*, 1709.
(12) (a) Yue, W.; Zhao, Y.; Shao, S. Y.; Tian, H. K.; Xie, Z. Y.; Geng, Y. H.; Wang, F. S. *J. Mater. Chem.* **2009**, *19*, 2199. (b) Chen, M.-H.; Hou, J. H.; Hong, Z. R.; Yang, G. W.; Sista, S.; Chen, L.-M.; Yang, Y. *Adv. Mater.* **2009**, *21*, 1.
(13) Lenes, M.; Wetzelaer, G. A. H.; Kooistra, F. B.; Veenstra, S. C.; Hummelen, J. C.; Blom, P. W. M. *Adv. Mater.* **2008**, *20*, 2216.
(14) Ross, R. B.; Cardona, C. M.; Guldi, D. M.; Sankaranarayananan, S. G.; Reese, M. O.; Kopidakis, N.; Peet, J.; Walker, B.; Bazan, G. C.; Keuren, E. V.; Holloway, B. C.; Grees, M. *Nat. Mater.* **2009**, *8*, 208.
(15) (a) Iqbal, A.; Jost, M.; Kirchmayr, R.; Pfenninger, J. A.; Rochat, A.; Wallquist, O. *Bull. Soc. Chim. Belg.* **1988**, *97*, 615. (b) Yamamoto, H. International Patent WO2004/090046, **2004**.
(16) Zhou, E. J.; Nakamura, M.; Nishizawa, T.; Zhang, Y.; Wei, Q. S.; Tajima, K.; Yang, C. H.; Hashimoto, K. *Macromolecules* **2008**, *41*, 8302.